VULNERABILITY OF TRAFFIC EMBANKMENTS TO LIQUEFACTION-INDUCED DEFORMATIONS

Aleš Oblak*, University of Ljubljana, Faculty of Civil and Geodetic Engineering, Chair of Geotechnical Engineering, Ljubljana, SLOVENIA, aoblak@fgg.uni-lj.si

Janko Logar, University of Ljubljana, Faculty of Civil and Geodetic Engineering, Chair of Geotechnical Engineering, Ljubljana, SLOVENIA

Sebastjan Kuder, University of Ljubljana, Faculty of Civil and Geodetic Engineering, Chair of Geotechnical Engineering, Ljubljana, SLOVENIA

Antonio Viana Da Fonseca, CONSTRUCT-GEO, Faculty of Engineering, University of Porto (FEUP), Porto, Portugal

ABSTRACT

Liquefaction-induced deformations on traffic embankments were studied using software package FLAC in combination with advanced material model PM4Sand in order to simulate the liquefaction phenomenon. A parametric study was carried out, where the geometry of the embankment and soil profile was varied. In addition, numerical analyses were performed for two sets of material properties of the liquefiable sandy layer – medium dense and loose state. On the basis of numerical results, fragility curves were derived in terms of crest settlement as damage state parameter and Arias intensity or peak ground acceleration as intensity measure.

Keywords: Embankment, Liquefaction, FLAC, Vulnerability Analysis.

1. INTRODUCTION

Soil liquefaction is a phenomenon where soil loses its shear strength and stiffness due to rearrangement of solid particles, which leads to a pore pressure build-up during dynamic loading, such us earthquakes. Most often, liquefaction occurs in loose saturated sandy to silty sandy soils. The development and extent of the consequences of this complex phenomenon depend on many factors. Initially, properties of a liquefiable layer, ground motion characteristics and site conditions (thickness and depth of layers susceptible to liquefaction, ground water level, ground inclination, etc.), along with other circumstances associated with the effects of human activities in the ground near the site under consideration.

According to literature ([1], [2] and [3]), earth dams, embankments and river levees are very vulnerable to seismic shaking and liquefaction occurrence under foundations. Within this study, attention was given to traffic embankments built on liquefiable ground, since they are of vital importance and represent links between assistant institutions and affected areas. A parametric study of an embankment was conducted using 2D finite difference program FLAC. Numerical simulation of liquefaction process in the ground was achieved using advanced PM4Sand material model [4]. Individual combination of model geometry and material properties was shaken by 30 ground motions with at least 8 different peak ground acceleration levels in order to derive fragility curves.

2. MODEL DESCRIPTION

2.1. Model geometry and material properties

The earthquake-liquefaction-induced deformations of traffic embankment were observed on a simple numerical model for four different soil profiles – S1, S2, S4 and S5. Soil profiles S1, S4 and S5 contain a liquefiable sandy layer of various thicknesses (7, 2 and 4 m, respectively), which lie between 24 m thick base stiff clay layer and 1 m thick clayey crust layer on top, while soil profile S2 was modelled with a 7 m thick liquefiable layer without crust. Ground water level was placed at one meter depth.

Considering embankment geometry, slope inclination was set to 1:2 (vertical:horizontal) and remained constant through all analyses. Additionally, embankment height was varied from 2 to 8 m by steps of 2 m and was analysed in combination with all soil profiles and 24 m wide embankment crest, whereas the effect of crest width (6, 12 and 24 m) was considered only for soil profile S1 and 4 m high embankment.

Basic model variables are presented in Figure 1 and Table 1.

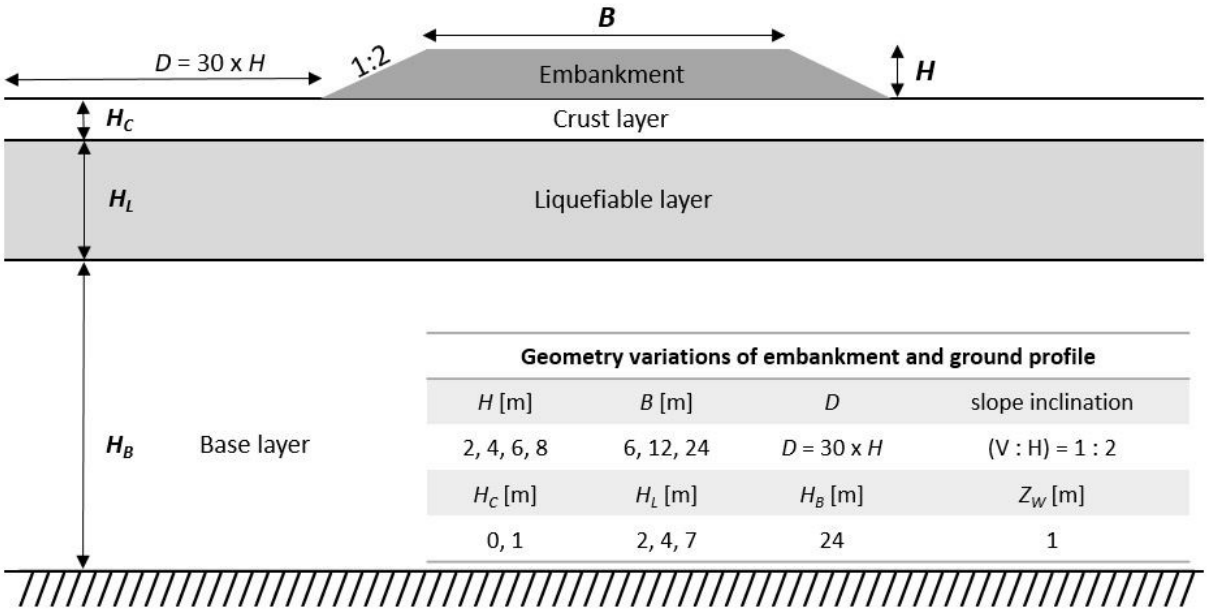

Figure 1. *Model geometry.*

Table 1. *Soil profiles.*

Soil ID	H_C – thickness of crust layer [m]	H_L – thickness of liquefiable layer [m]	H_B – thickness of base layer [m]
S1	1	7	24
S2	0	7	24
S4	1	2	24
S5	1	4	24

The numerical model was constructed in several phases. Firstly, free field initial stresses were calculated after the geometry, material parameters, pore water pressure distribution and boundary conditions for static analysis had been assigned to the model. Then followed the construction of the embankment and the replacement of the material model. It was assumed that only sandy layer can liquefy; thus, PM4Sand model was assigned to that layer only. Other layers were modelled by Mohr-Coulomb material model throughout the analysis. In the next

phase, seismic load was applied to the model. For this purpose, free field boundary condition at lateral edges and compliant base at the bottom of the model was set. Ground motion was transformed into shear stress history and applied at the compliant base.

Since numerical analyses were carried out for hypothetical ground conditions, all secondary input parameters for PM4Sand material model were kept at their default values. The three main input parameters (relative density – D_r, shear modulus coefficient – G_0 and Contraction rate parameter – h_{po}) were selected on the basis of real soil tests.

Material properties for three soil layers and embankment are presented in Table 2.

Table 2. *Material properties.*

Layer	Dry density	Bulk modulus	Shear modulus	Undrained shear strength	φ'	c'	PM4Sand		
	kg/m^3	MPa	MPa	kPa	°	kPa	D_r [/]	G_0 [/]	h_{po} [/]
Crust	1784	64	30	80	-	-	-	-	-
Liquefiable "loose"	1486	57.3	43	-	30	0	0.6	760	0.55
Liquefiable "medium"	1486	77	77	-	30	0	0.35	476	0.5
Base	1436	227	105	150	-	-	-	-	-
Embankment	1800	83.3	38.5	-	35	5	-	-	-

Two sets of sandy layer characteristics were analysed within this study, depending on the density of the liquefiable layer – medium dense and loose state, with relative density equal to 0.6 and 0.35, respectively. Liquefiable layer was underlain by stiff clay with undrained shear strength of 150 kPa.

2.2. Ground motions

A selection of 30 real acceleration time histories recorded on rock outcrop were used as dynamic loading in numerical calculations. Ground motions (GM) were collected from PEER (Pacific Earthquake Engineering Research Center) database in such manner that the mean spectrum of the selected ground motions matches sufficiently well the EC8 spectrum for soil class A, taking into account peak ground acceleration (PGA) of 0.25 g. All of 30 GMs were subsequently modified to different intensity levels for the derivation of fragility curves. In case of medium dense sand, eight intensity levels (0.25 g, 0.375 g, 0.5 g, 0.625 g, 0.75 g, 1.0 g, 1.25 g and 1.5 g) were used. For the loose case, three to four extra PGA levels were added (0.1 g, 0.2 g, 0.3 g and in some cases even 0.15 g). With these extra intensity levels, the whole range of fragility curves is sufficiently well covered by numerically calculated points, even in cases where crest deformations, and consequently the number of cases exceeding certain limit state, increase rapidly with increasing PGA at bedrock by small increments.

3. VULNERABILITY ANALYSIS AND RESULTS

Based on the results of numerical calculations, a vulnerability assessment of the traffic embankments was performed. The probability of exceedance of a certain limit state for the embankments in question is expressed by the means of fragility curves. Various approaches for the derivation of fragility curves can be found in literature, from empirical [5] and analytical [6] procedure to expert judgement or hybrid method. Within this study, analytical

approach was used due to the repeatability of numerical analyses on the same model subjected to different ground motions. In this way, the impact of uncertainties originating from the earthquake source is decreased.

Soil-structure interaction is very complex in case of traffic embankments underlain by liquefiable layer leading to several possible failure mechanisms – lateral spreading, subsidence of the crest, slope instability or hydraulic heave through cracks [7]. Since crest settlement is still widely used among geotechnical engineers due to its simple comparisons with field measurements, it was selected as engineering damage state parameter in this study, as well as in other relevant researches [8]. Permanent vertical displacement was obtained at the midpoint of embankment model. On the other hand, two different intensity measures were chosen – peak ground acceleration and Arias intensity. The first one is more commonly used in practice due to numerous correlations with other engineering parameters, while the latter more specifically describes the released energy during ground movement.

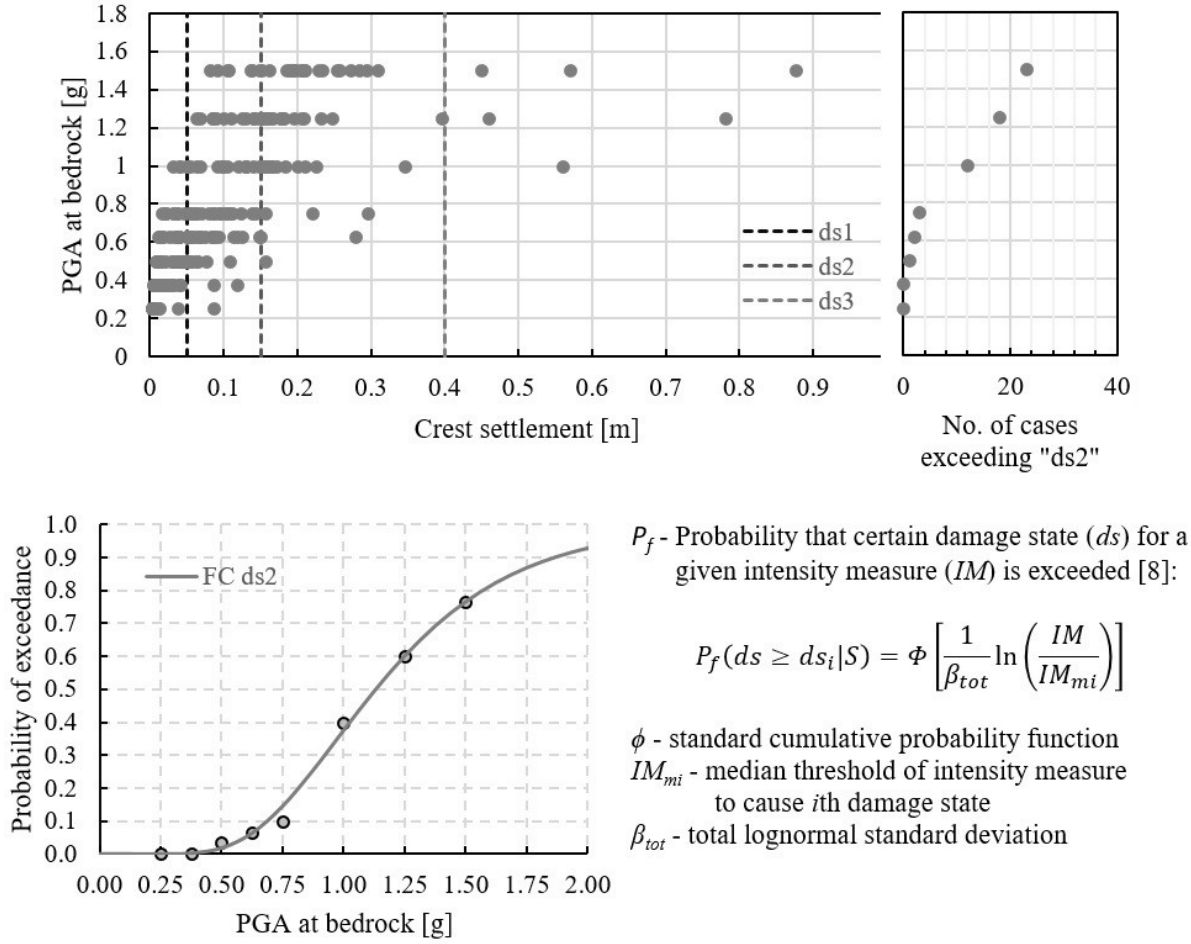

Figure 2. *Multiple Stripe Analysis procedure.*

Numerical analyses were performed following the principle of Multiple Stripe Analysis method [9], where calculations were executed at discrete intensity measure levels for a set of selected ground motions (see the example in Figure 2). The probability of exceedance was calculated as a number of cases exceeding certain limit state divided by the number of all performed analyses at *i*-th intensity level. Maximum of likelihood function was used for fitting procedure. Threshold values for the limit state parameter were gathered from literature [10] and are presented in Table 3.

Table 3. *Threshold values of damage states for highway and railway embankments [10].*

Damage state	Permanent vertical ground displacement [m] – **highway**			Damage state	Permanent vertical ground displacement [m] – **railway**		
	min	max	mean		min	max	mean
ds1 – minor	0.02	0.08	**0.05**	**ds1** – minor	0.01	0.05	**0.03**
ds2 – moderate	0.08	0.22	**0.15**	**ds2** – moderate	0.05	0.10	**0.08**
ds3 – extensive	0.22	0.58	**0.40**	**ds3** – extensive	0.10	0.30	**0.20**

Typical numerical results in terms of permanent displacements at final calculation step, progress of crest settlements through dynamic time, are introduced in the subsections below. Furthermore, the effects of different model variations (embankment height, crest width, thickness of liquefiable layer, presence of crust layer and density state of liquefiable layer) are presented through fragility curves below.

3.1. Numerical results – embankment displacements

Typical distribution of the embankment`s displacements at the end of analysis and advancement of crest settlement at midpoint with time are shown in Figure 3. The figure below represents a case with 6 m high embankment, underlain by crust layer and 7 m thick medium dense liquefiable layer (soil profile S1), subjected to dynamic loading with PGA at bedrock equal to 1.0 g. Actual values of calculated displacements depend on selected ground motion, because earthquake records with various frequency compositions and time durations are considered within the set of 30 GMs.

Generally, rotational slip surface at both sides, crest subsidence and lateral spreading in horizontal direction due to dynamic excitation and consequent foundation`s liquefaction, were observed in the majority of numerical calculations. Similar failure mechanism was noticed in literature [11, 12]. The detailed exploration of all deformed shapes of the analysed embankments is beyond the scope of this paper.

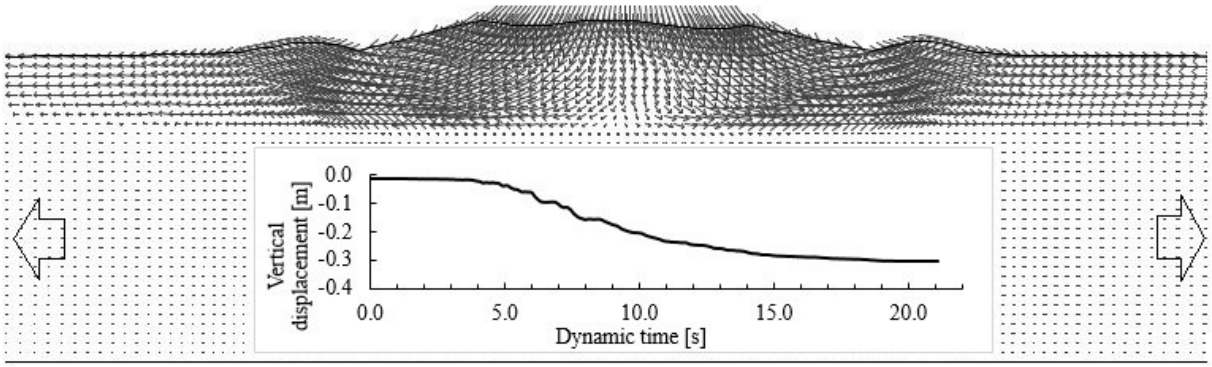

Figure 3. *Typical deformed shape of the embankment and settlement vs. time during shaking.*

3.2. Fragility curves

The outcomes of the vulnerability analysis of traffic embankments are expressed through fragility curves (see Figure 4 to Figure 7). Fragility curves under this study were derived based on permanent vertical crest settlements in the midpoint of the model, where mean threshold values of damage states for traffic embankments from Table 3 were used. Three limit states were considered – minor (ds1), moderate (ds2) and extensive (ds3).

With the aim of achieving sufficient clarity in the figures containing fragility curves, different line types are used to differentiate between model variations (crest width, embankment height, thickness and density state of the liquefiable layer), while the damage states differ in colour, namely ds1 (light grey), ds2 (dark grey) and ds3 (black).

In addition, Figure 4 and Figure 5 are based on damage states for highways, while Figure 6 and Figure 7 present fragility curves for railways. Regardless of the choice of threshold values for limit states, the trends of various effects related to the model variations are the same, only the curves move to the left, due to more rigorous criteria for railways.

3.2.1. Influence of crest width

According to Figure 4, lower settlements in the middle point are expected with increasing crest width, based on three examined cases (6 m, 12 m and 24 m). Analyses were performed on a case with a 4 m high embankment underlain by soil profile S1 with medium dense sandy layer.

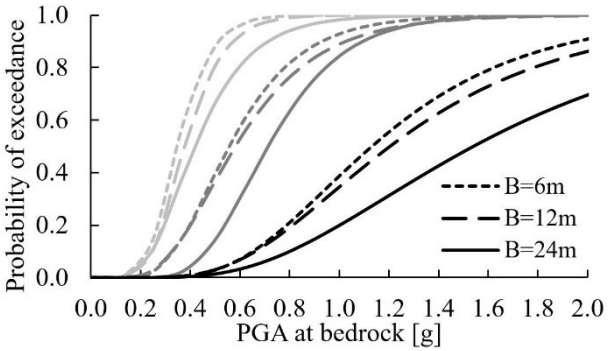

Figure 4. *Effect of crest width on fragility curves (highway criteria) – ds1, ds2 & ds3.*

3.2.2. Influence of embankment height

The impact of the height of embankment was analysed on the model with 24 m wide crest, where embankment was built on soil profile S1. Both Figure 5a and Figure 5b show that vulnerability of the embankment rises with increasing embankment height, since the curves move to the left.

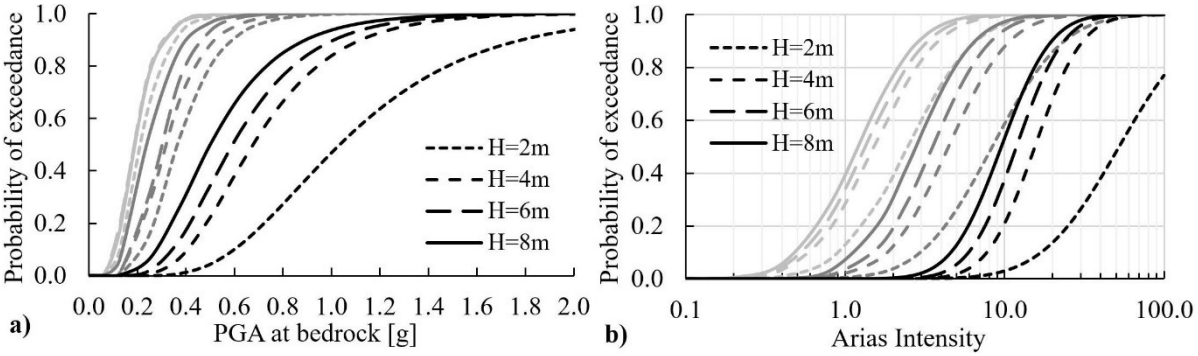

Figure 5. *Effect of embankment height on fragility curves (highway criteria) for a) PGA and b) Arias Intensity – ds1, ds2 & ds3.*

3.2.3. Influence of thickness of liquefiable layer

The effects of the thickness of liquefiable layer and the presence of crust layer were studied on a model with 6 m high embankment and 24 m wide crest. Moreover, soil properties related to the medium dense case were assigned to the sandy layer.

Initially, larger settlements were expected with increasing thickness of liquefiable layer. Figure 6 clearly shows that this is partially true, because the probability of exceeding certain limit state is greater in the case of a 7 m than in the case of a 4 m thick liquefiable layer. Even larger probability was calculated for the case without crust layer and 7 m thick sandy layer. Nevertheless, greater vulnerability was obtained for the case with soil profile S4 (H_L = 2 m) compared to S5 (H_L = 4 m) for this particular model variation.

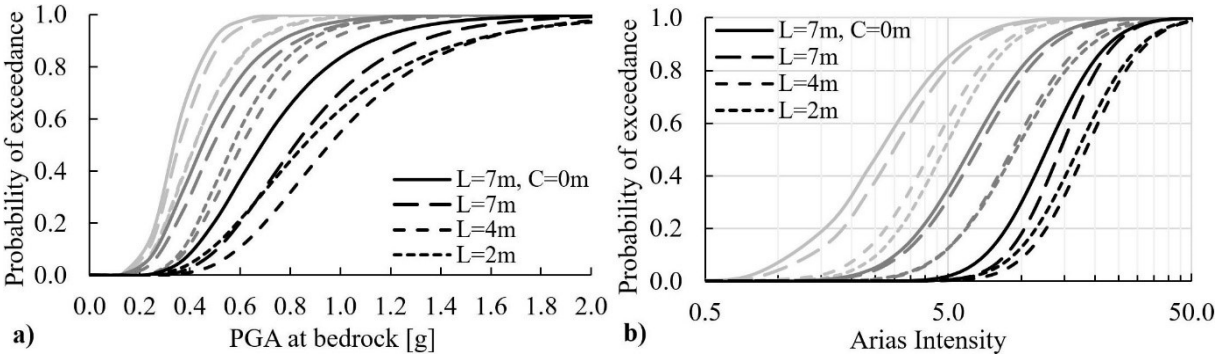

Figure 6. *Effect of thickness of liquefiable layer (railway criteria) for a) PGA and b) Arias Intensity – ds1, ds2 & ds3.*

3.2.4. Influence of density of liquefiable layer

Model with a 6 m high embankment and 24 m wide crest, lying on soil profile S2, was used for the comparison between loose and medium dense state of the liquefiable layer. The result is presented in Figure 7, where larger crest settlements were calculated for the loose case.

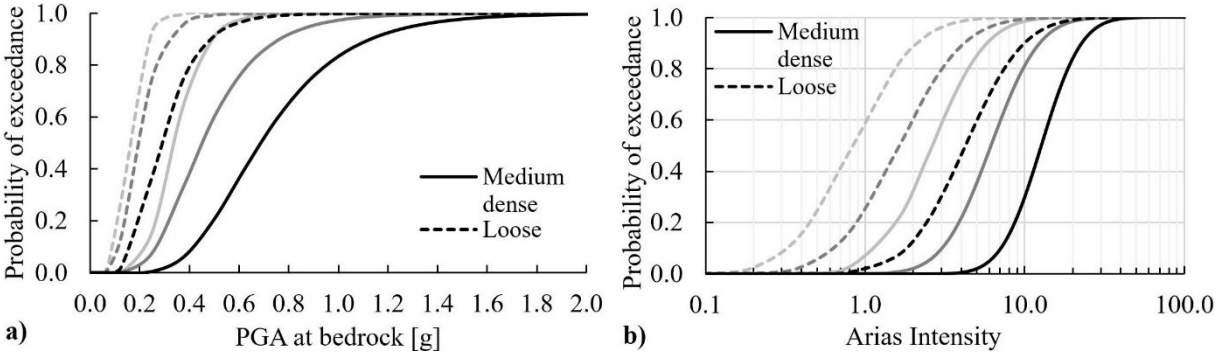

Figure 7. *Effect of soil density on fragility curves (railway criteria) for a) PGA and b) Arias Intensity – ds1, ds2 & ds3.*

4. CONCLUSION

A comprehensive set of numerical calculations of the traffic embankment built on liquefiable ground was made using 2D FLAC software in order to perform the vulnerability analysis. The soil behaviour during liquefaction was captured with advanced PM4Sand material model. Attention was given to the deformation of the embankment crest, more precisely, permanent vertical displacement at midpoint was used as damage state parameter for the derivation of fragility curves. Fragility curves were determined for different variations of the model parameters, among which crest width, embankment height, presence of crust layer, density state and thickness of liquefiable layer were varied. Uncertainties related to earthquake excitation were decreased using a set of 30 ground motions recorded on rock outcrop. Depending on the case, ground motions were scaled to at least 8 intensity levels until the entire range of the fragility curve was reasonably well covered. On the basis of numerical calculations and figures presented above, it was found out that the probability of exceeding certain limit state for the studied range increases with increasing embankment height (2 m, 4 m, 6 m and 8 m) or with decreasing crest width (6 m, 12 m and 24 m). Furthermore, depending on the density state of the liquefiable layer, greater deformations at the embankment crest are expected for looser sand. The effect of thickness of the liquefiable layer is not so straightforward, since it turned out that the embankment is more vulnerable if built on soil profile S4 (H_L = 2 m) than on soil profile S5 (H_L = 4 m), but less than on soil profile

S1 (H_L = 7 m). Nonetheless, absence of crust layer causes larger crest settlement, when comparing embankment deformations built on soil profiles S1 and S2. Fragility curves were derived based on damage criteria from literature [10] for highway and railway embankments. Additional information can be found in [13].

ACKNOWLEDGEMENT

This study is a product of the LIQUEFACT project, funded by the European Union`s Horizon 2020 research and innovation programme under grant agreement No GAP-700748.

REFERENCES

[1] Siyahi, B., Arslan, H., 2008. *"Earthquake induced deformation of earth dams"*, Bulletin of Engineering Geology and the Environment, 67(3):397-403, DOI: 10.1007/s10064-008-0150-5.

[2] Wu, G., 2014. *"Seismic Design of Dams"*, Encyclopedia of Earthquake Engineering, 1-18, DOI 10.1007/978-3-642-36197-5_96-1.

[3] Argyroudis, S., Mitoulis, S., Kaynia, A.M., Winter, M.G., 2018. *"Fragility Assessment of Transportation Infrastructure Systes Subjected to Earthquakes"*, Geotechnical Earthquake Engineering and Soil Dynamics V GSP, 174-183, 10-13 June 2018, Austin, Texas, USA.

[4] Boulanger, R.W., Ziotopoulou, K., 2017. *"PM4Sand (Version 3.1): A sand Plasticity Model for Earthquake Engineering Applications*", Report No. UCD/CGM-17/01.

[5] Maruyama, Y., Yamazaki, F., Mizuno, K., Tsuchiya, Y., Yogai, H., 2010. *"Fragility curves for expressway embankments based on damage datasets after recent earthquakes in Japan"*, Soil Dynamics and Earthquake Engineering, 30(11): 1158-1167, doi.org/10.1016/j.soildyn.2010.04.024.

[6] Khalil, C., Rapti, I., Lopez-Caballero, F., 2017. *"Numerical Evaluation of Fragility Curves for Earthquake-Liquefaction-Induced Settlements of an Embankment"*, Geo-Risk 2017, pp. 21-30, 4-7 June 2017, Denver, Colorado, USA.

[7] Rapti, I., Lopez-Caballero, F., Modaressi-Farahmand-Razavi, A., Foucault, A., Voldoire, F., 2018. *"Liquefaction analysis and damage evaluation of embankment-type structures"*, Acta Geotechnica, 13(5): 1041-1059, doi.org/10.1007/s11440-018-0631-z.

[8] Argyroudis, S., Kaynia, A.M., 2015. *"Analytical seismic fragility functions for highway and railway embankments and cuts"*, Earthquake Engineering & Structural Dynamics, 44(11): 1863-1879.

[9] Baker, J.W., 2015. *"Efficient Analytical Fragility Function Fitting Using Dynamic Structural Analysis"*, Earthquake Spectra, 31(1): 579-599, doi.org/10.1193/021113EQS025M.

[10] Pitilakis, K. (project coordinartor), Kaynia, M.A. (report editor), 2009-2013. *"Fragility curves for all elements at risk"*, Systemic Seismic Vulnerability and Risk Analysis for Buildings, Lifeline Network and Infrastructures Safety Gain (SYNER-G), Project N°: 244061, Call N°: FP7-ENV-2009-1.

[11] Maharjan, M., Takahashi, A., 2014. *"Liquefaction-induced deformation of earthen embankments on non-homogenous soil deposits under sequential ground motions"*, Soil Dynamics and Earthquake Engineering, 66: 113-124, DOI: 10.1016/j.soildyn.2014.06.024.

[12] Oka, F., Tsai, P., Kimoto, S., Kato, R., 2012. *"Damage patterns of river embankments due to the 2011 off the Pacific Coast of Tohoku Earthquake and a numerical modeling of the deformation of river embankments with a clayey subsoil layer"*, Soils and Foundations, 52(5): 890-909, doi.org/10.1016/j.sandf.2012.11.010.

[13] Viana da Fonseca et al. (2018). "*Methodology for the liquefaction fragility analysis of critical structures and infrastructures: description and case studies*", LIQUEFACT Deliverable D3.2, Horizon 2020 EU funding for Research & Innovation Project ID: 700748 (www.liquefact.eu).